COBEM 2021 26th International Congress of Mechanical Engineering
November 22-26, 2021, Virtual Congress, Brazil

COB-2021-1891
TRANSIENT THERMAL DIFFUSION AND TEMPERATURE DISTRIBUTION OF A CYLINDRICAL FUEL PELLET SHIFTED RADIALLY IN PRESSURIZED WATER REACTOR

Felipe Ferreira Timoteo
Thiago Figueiral Ribeiro Dias da Rosa
Marcos Filardy Curi
Centro Federal de Educação Tecnológica Celso Suckow da Fonseca, Department of Mechanical Engineering
Rodovia Mário Covas, lote J2, quadra J, Rio de Janeiro, CEP: 23812-101, Brazil
marcos.curi@cefet-rj.br

Abstract. *In recent years, the rising demand for carbon-free energy sources makes alternative sources, such as nuclear energy, a promising solution to do away with the effects on long-term climate changes, reducing greenhouse effect gases in electricity generation. Notwithstanding, the nuclear solution must overcome high construction costs and safety risks to succeed. The thermodynamics and heat transfer inside the reactor core is physically and mathematically complex to simulate or predict based on non-linear governing equations. In this regard, this paper aims to investigate the radial thermal diffusion and temperature distribution of the fuel rod of a pressurized water reactor (PWR) using finite element modelling technique (FEM). This study first conducted a steady-state analysis considering temperature-dependent parameters as gap conductance approximation, density, thermal capacity, the thermal conductivity of the fuel pellet and clad, and a uniform volumetric heat-generation rate. Geometric characteristics of Westinghouse AP1000 were also implemented. In addition, a transient analysis of the fuel rod is developed to evaluate the effect of the cylindrical fuel pellet shifted radially. The temperature profiles of the fuel pellet and clad resulting from FE analysis shows important maximum temperature spots as the outside surface of the fuel and the inner surface of the clad.*

Keywords: *Fuel pellet, Shifted Radially, PWR, AP1000, Steady-state, Transient-state*

1. INTRODUCTION

With the growing demand for electricity and the constant search to reduce greenhouse gas emissions, power generation by nuclear sources stands out to produce clean energy. However, nuclear reactors, like other generation systems, present inherent risks. The accidents of Chernobyl (1986, Soviet Ukraine) and Fukushima 1 (2011, Japan) are well-known examples. However, the risks associated with nuclear generation are extremely low compared to other work systems. From this standpoint, nuclear generators are one of the ways of producing large amounts of electrical power without much harm to the environment (Lamarsh and Baratta, 2001). In this context, an accurate description of the temperature distribution in fuel elements is essential to predict the lifetime behavior of core structural materials (Todreas and Kazimi, 2011).

In a nuclear reactor, the heat transfer process between the fuel rod and the cooling fluid has great importance to predict the core components behavior and It is, consequently, crucial for safety assurance. Conversely, knowing the temperature distribution in the fuel rod in a steady-state by the analytical procedure is a difficult task. Furthermore, the complexity of the phenomena increases when a transient state is taken into consideration and when the main physical parameters of the pellet and clad such as thermal conductivity, density and thermal capacity are set to be temperature-dependent to represent the real operational condition.

For this reason, the finite element modeling approach (FEM) was utilized to investigate temperature distribution in a fuel pellet out-of-center positioned inside the tubular clad protection. Such a condition is caused by turbulent flow-induced vibrations which lead to a relative motion between the fuel pellet and the cladding (D'Ambrosi, 2021) that shortens the gap in some locations and consequently changes the temperature profile radially once the thermal resistance is modified locally.

The fuel rod dimensions were based on the Westinghouse AP1000 pressurized water reactor (PWR) to produce real-life engineering results and conclusions. The PWR type was chosen due to the amount of data available and due to the fact that pressurized water reactors are the most popular project type in this century, and they are responsible for two-thirds of the nuclear-installed capacity in the world (Kok, 2017). The study analyzed the rod in the steady-state and

transient state with the pellet centered and with a convective boundary condition applied to the external surface of the clad protection tube. Following this, the pellet was geometrically shifted radially and steady state and transient analysis were done again.

2. METHODOLOGY

Based on Newton and Fourier's laws (Incropera *et al*., 2008), and considering the temperature-dependent material properties of the fuel rod, this section will provide all the parameters and details used in the FEA model for the AP1000 reactor study. According to (Todreas and Kazimi, 2011), under certain conditions, the neutron and temperature fields can be decoupled and, thus, assuming that the energy deposition rate is known, it is possible to obtain the radial temperature profile on the rod. The outer surface convective coefficient of the cladding was determined according to (El-Wakil, 1971) and (Westinghouse, 2011) for the axial position of the rod. In addition, the stationary and transient analysis considered a non-irradiated fuel pellet with the largest possible gap thickness.

$$T_{coolant}(z) = T_{in} + \frac{q_0^{'''} r_{fuel}^2 L}{Cp\dot{m}} \left(1 - cos\left(\frac{\pi}{2} + \frac{\pi z}{L}\right)\right), \tag{1}$$

$$\frac{hD_e}{K} = 0.023 \left(\frac{D_e G}{\mu}\right)^{0.8} \left(\frac{C_p \mu}{K}\right)^{0.4}, \tag{2}$$

where $T_{coolant}$ is the coolant mean temperature, T_{in} is the coolant mean temperature in the channel inlet, $q_0^{'''}$ is the volumetric heat generation rate, r_{fuel} is the fuel radius, L is the effective core length, D_e is the equivalent diameter, Cp is the specific heat of the coolant, $\dot{m}$ is the coolant mass flow in the channel and G is the mass velocity of the coolant from (Costa, 2017), the z is the axial position from the fuel rod center, μ is the dynamic viscosity of the coolant, K is the thermal conductivity and h is the convective heat transfer coefficient. Once the temperature of the coolant on the fuel rod center axial position is acquired from Eq. 1, it is possible to calculate, using the water coolant's physical properties for the given temperature found in (NIST, 2021), the heat transfer coefficient h utilizing Eq. 2. These properties are shown in Table 1.

2.1 Fuel Pellet

Inside the fuel pellet is where the fission process of the uranium nuclei occurs and the chain reaction is sustained to produce heat converted into electricity. Following (Westinghouse, 2011) the fuel pellets are circular cylinders made of enriched uranium-dioxide powder compacted by cold pressing and finally sintered until the target density. Those pellets are stacked inside a tubular clad protection to form the fuel rod.

The volumetric heat generation rate ($q^{'''}$) can be obtained by the Eq. 3 from (Todreas and Kazimi, 2011), where Q_{linear} is the linear power rate of 18770 W/m from (Westinghouse, 2011), L_e is the extrapolated core length, r_{fuel} is the fuel radius available in Table 1 and z is the axial coordinate of the fuel rod being the origin positioned at the center. In addition, Eq. 4 (Martin, 1988), Eq. 5 (Lucuta *et al.* , 1996) and Eq. 6 (Newman, 2009) model fuel density (ρ_{UO_2}), thermal capacity (Cp_{UO_2}) and thermal conductivity (k_{UO_2}) respectively.

$$q^{'''}(z) = \frac{Q_{linear}}{\pi r_{fuel}^2} . cos\left(\frac{\pi z}{L_e}\right), \ -L/2 \leq z \leq L/2, \tag{3}$$

$$\rho_{UO_2} = 10960(a + bT + cT^2 + dT^3), \tag{4}$$
$$273 \leq T \leq 923K (a = 0.997, b = 9.082 \cdot 10^{-6}, c = -2.705 \cdot 10^{-10}, d = 4.391 \cdot 10^{-13}),$$
$$923 \leq T \leq 3120K (a = 0.997, b = 1.179 \cdot 10^{-5}, c = -2.429 \cdot 10^{-9}, d = 1.219 \cdot 10^{-12}),$$

$$Cp_{UO_2} = 264.26 + 0.047T, \tag{5}$$

$$k_{UO_2} = \frac{1}{0.0375 + 2.165 \cdot 10^{-4} T} + \left(\frac{4.715 \cdot 10^9}{T^2}\right) e^{\left(\frac{-16.361}{T}\right)}. \tag{6}$$

2.2 Gap

On a fuel rod, a space is provided between the UO_2 pellet and the cladding. Initially, this space is filled with helium at a certain pressure that depends on the type of core and the operating conditions of the reactor. To determine the temperature distribution in the radial direction, it was assumed an as-fabricated condition, that is, with the gap in its largest thickness and smallest gap conductance (Fenech, 1981). The heat transfer in the gap was treated purely by conduction as in Tang *et al*. (2017), even though in the case of an inert gas layer the heat transfer between the fuel and the cladding occurs by conduction, thermal radiation and convection (Lanning and Hann, 1975). Furthermore, it was assumed that density and thermal conductivity are dependent on temperature and specific heat under constant pressure (Mihaila *et al*., 2009). In addition, Eq. 7, 8 and 9 (Bejan, 1993) model gap density (ρ_{He}), thermal capacity (Cp_{He}) and thermal conductivity (k_{He}) respectively.

$$\rho_{He} = 0.0818 - 8.275 \cdot 10^{-5}(T - 600), \tag{7}$$

$$Cp_{He} = 5190.0, \tag{8}$$

$$k_{He} = 0.0468 + 3.81 \cdot 10^{-4}T - 6.79 \cdot 10^{-8}T^2. \tag{9}$$

2.3 Cladding

The fuel rod cladding is the first barrier to the release of radioactivity in a nuclear reactor. This cladding is usually made of a zirconium alloy or stainless steel. In the AP1000 reactor the cladding is made of a zirconium alloy called ZIRLO developed by Westinghouse. This material is an evolution of earlier zirconium alloys that presents greater resistance to corrosion, fuel temperature and higher burnup rates (Westinghouse, 2016). In addition, Eq. 10, Eq. 11 (Hagrman, 1995) and Eq. 12 (IAEA, 2006) model the zirconium cladding density ($\rho_{zircaloy}$), thermal capacity ($Cp_{zircaloy}$) and thermal conductivity ($k_{zircaloy}$) respectively.

$$\rho_{zircaloy} = 6490.0, \tag{10}$$

$$Cp_{zircaloy} = 255.66 + 0.1024T \ (273 < T < 1100K), \tag{11}$$

$$k_{zircaloy} = 7.51 + 2.09 \cdot 10^{-2}T - 1.45 \cdot 10^{-5}T^2 + 7.67 \cdot 10^{-9}T^3. \tag{12}$$

3. Finite Element Modeling

The geometry analyzed consisted of three main domains, a central cylindrical solid to represent the UO_2 fuel pellet, the gap layer and the cladding. When the pellet is centered, the physical problem is axisymmetric. Due to this fact, only one-eighth of the model is represented in order to save computer processing power. However, when the pellet is shifted radially, a model sliced in half is required since the azimuthal symmetry is no longer present. Figure 1.a shows the sliced geometry, the directions and the domains for AP1000, where r_{fuel} is 4.096 mm, r_{gap} is 4.178 mm and r_{clad} is 4.750 mm (Westinghouse, 2011).

The model mesh was constructed mainly with a hexahedral SOLID70 ANSYS element with eight nodes with one temperature degree of freedom in each node. Note in Figures 1.b and 1.c, that there is a gross discretization in the axial direction. This configuration was chosen because the heat generation rate was considered constant along this direction of the fuel rod partition analyzed. Therefore, this dimension is only for representative purposes in the present study. Figure 1.b shows the mesh of a one-eighth slice of the fuel rod utilized in pellet-centered analysis while Figure 1.c shows the mesh of the half-sliced fuel rod with the pellet shifted radially. It is important to highlight that the gap intentionally presents more than two elements in thickness to better capture the temperature gradient. It is also worth mentioning that the half model was re-meshed for each case of shifted pellet and the mesh presented in Figure 1.c is a sample of the cases analyzed. Also, a mesh convergence study was performed to ensure that the mesh size does not impact the temperature results throughout the fuel rod. Table 2. shows four different mesh densities that were

implemented in ANSYS and how it influences the maximum temperature. It was observed to change less than 0.01 K in mesh 04.

Two different axial points of the fuel rod were analyzed, one being the axial center and the other being the fuel rod end positioned at the exit of the coolant fluid path. For both transient and steady state analysis the heat generations of 3.5621e+08 W/m³ for the fuel rod axial center and 3.8525e+07 W/m³ for the fuel rod axial exit calculated by Eq. 3 were assigned to the pellet while the external surface of the cladding received convection with heat transfer coefficient of 37023 W/m².K for the fuel rod center analysis and 39401 W/m².K for the fuel rod exit calculated by Eq. 2 for the bulk temperature of 587 K and 606K respectively. Figure 2 shows the applied conditions with flag A and B respectively.

Table 1. Physical Properties utilized in this study.

Properties			
Variables	Description	Center (1)	Exit (2)
T_{in}	Temperature in the channel inlet, K	552.59	-
$T_{coolant}$	Coolant mean temperature, K	587	606
q'''	Volumetric heat generation rate, W/m³	3.5529e+08	3.8525e+07
L	effective core length, m	4.2672	-
z	Axial position at fuel rod axial, m	0	2.1336
D_e	Equivalent diameter, m	0.0118	-
L_e	Extrapolated core length, m	4.5832	-
r_{fuel}	Fuel radius, m	4.096e-03	-
r_{Gap}	Outside gap radius, m	4.178e-03	-
r_{Clad}	Outside clad radius, m	4.750e-03	-
Cp	Specific heat of the coolant, J/kg.K	5884.2	7043.9
$\dot{m}$	Coolant mass flow in the channel, kg/s	0.3152	-
G	Mass velocity of the coolant in the channel, kg/s.m²	3458.6	-
μ	Dynamic viscosity of the coolant, Pa.s	8.2979e-05	7.4700e-05
K	Thermal conductivity, W/m.K	0.5344	0.4900
h	Convective Heat transfer coefficient, W/m².K	37023	39401

(1) Measured at 15.375 MPa.
(2) Measured at 15.238 MPa.

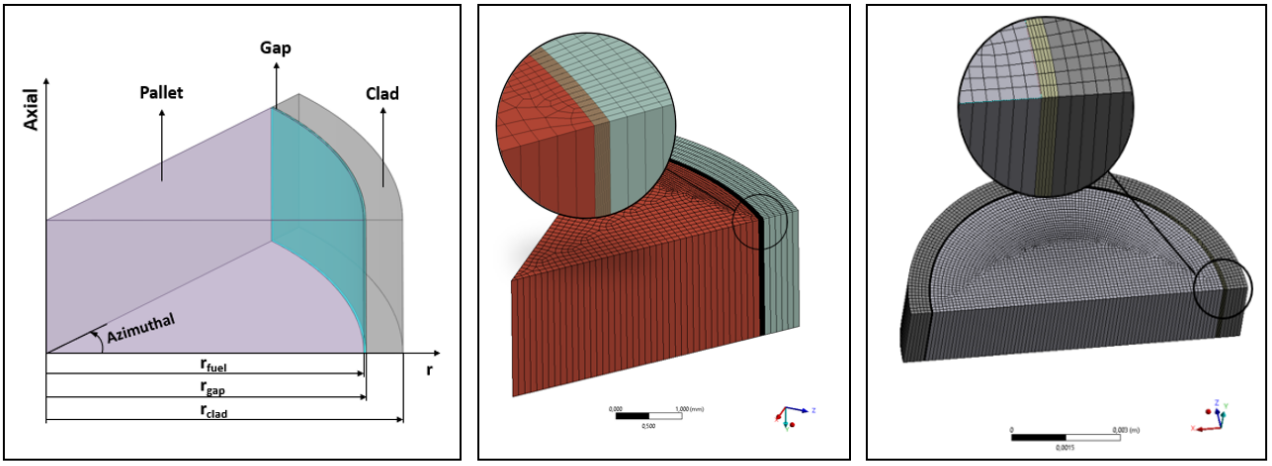

Figure 1. (a) Rod geometry, (b) one-eighth sliced meshed geometry and (c) Half-sliced pellet shifted meshed geometry .

Table 2. Mesh convergence analysis.

Mesh	Number of nodes	Maximum temperature
Mesh 01	7942	1236.45 K
Mesh 02	15974	1236.75 K
Mesh 03	30698	1236.76 K
Mesh 04	84222	1236.76 K

4. Results and Discussion

4.1 Steady-state

Figure 2 shows the summarized results for the cases in which the pellet is centered and those where it has been shifted radially. The graph in Figure 2.a shows the temperature profile for various shifted dimensions. It can be noted that on the left side of the graph, where the fuel becomes close to the clad protection, the fuel wall temperature approximates to the temperature value on the cladding's inner wall. Consequently, on the right side of the graph a higher temperature value on the fuel wall can be observed when compared to the centered pellet temperature profile. In the same graph, it can be noted that while the pellet moves to the left the maximum temperature spot moves in the opposite direction. This phenomena can be explained by decrease of thermal resistance where the gap is shortened, which intensifies the heat flux, leading to a higher temperature gradient between the fuel center and its wall, and the increase of the thermal resistance where the gap is thickened that induces higher temperature spot to be shifted to this side due to the diminished heat flux, consequently a lower temperature gradient.

Figure 2.b shows the temperature change for different spots for each radial shift length analyzed in respect to the centered pellet results. It is possible to observe that the major change occurs on the fuel pellet while the temperature change on the cladding is almost negligible. It is important to highlight that the maximum temperature on the fuel decreases with the increase of shift length. This behavior can also be explained by the thermal resistance change. In cylindrical coordinate problems the increase of thermal resistance in one side of the fuel rod is followed by a decrease on the other side but not by the same amount, i.e. this change is not linear, but proportional to a logarithmic expression (Incropera *et al.*, 2008). Due to this fact, when compared to the pellet centered, the thermal resistance of the shifted pellet problem is smaller what leads to a better heat transfer condition, i.e. higher heat flux from the pellet, consequently leading to lower maximum temperatures on the pellet.

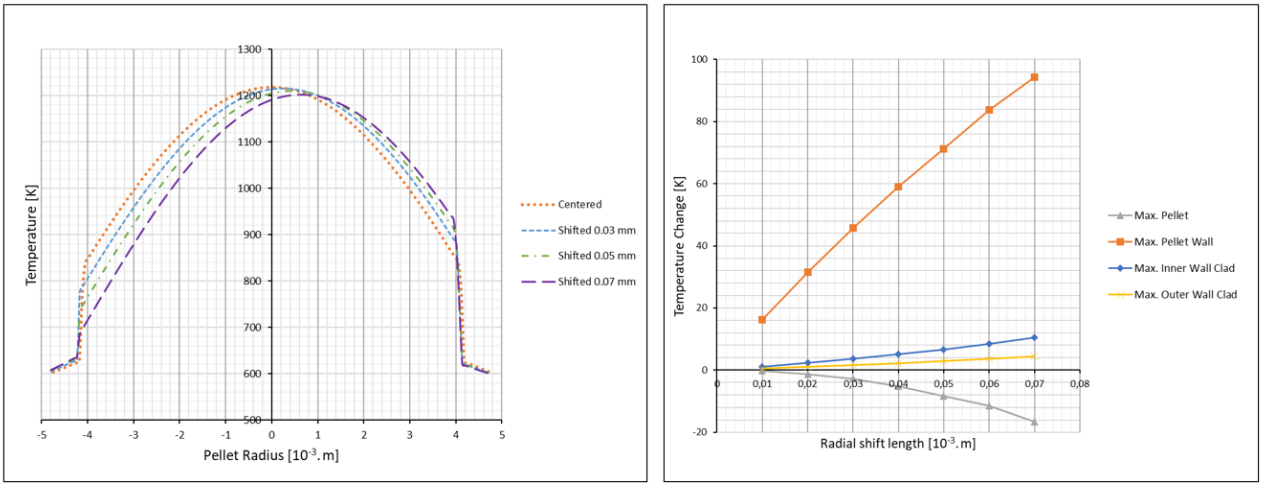

(a) (b)

Figure 2. (a) Temperature profiles for shifted dimensions for the fuel rod center ($z = 0$) and (b) Temperature change for the fuel rod center ($z = 0$).

Figure 3 shows a similar analysis for the final position of the rod ($z = 2.1336m$). In this case, the graph in Figure 3.a shows a reduction in the temperature of the entire pellet as a consequence of reduced volumetric heat generation and increased convection at that point. The graph in Figure 3b. shows the same behavior noted for the fuel rod center region but with smaller temperature gradients.

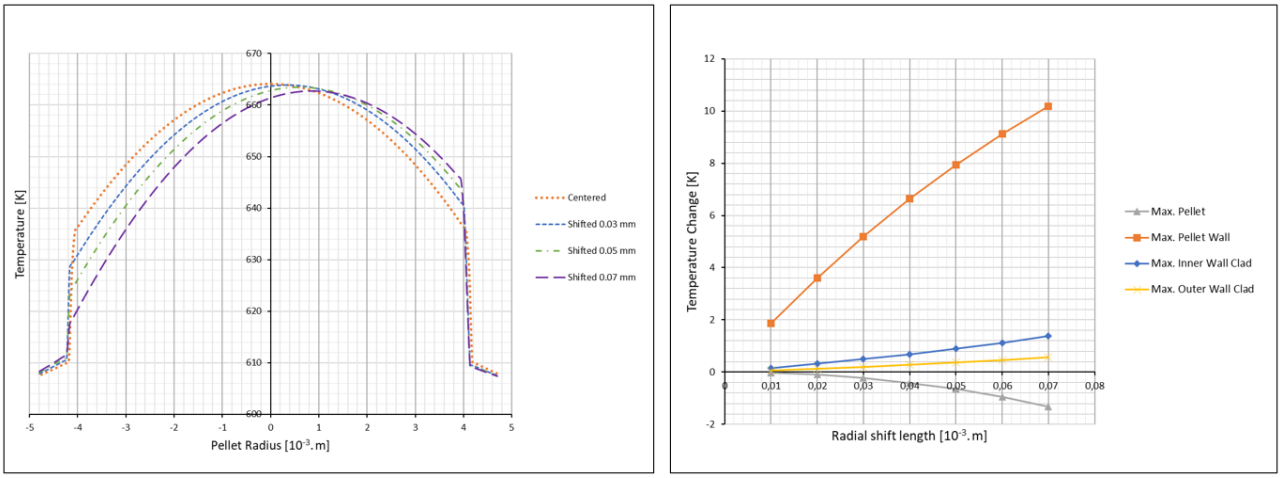

(a) (b)

Figure 3. (a) Temperature profiles for shifted dimensions for the fuel rod exit ($z = 2.1336m$) and (b) Temperature change for the fuel rod exit ($z = 2.1336m$).

4.2 **Transient-state**

Figure 4 shows the summarized results over time for the cases in which the pellet is centered and for those in which it has been shifted radially. The graph in Figure 4.a shows the maximum temperature on the fuel pellet for the fuel rod center ($z = 0$). It is possible to note that up to the ten-seconds mark the difference among the cases is not evident. Figure 4.b shows the maximum temperature over time for the fuel wall for the fuel rod center ($z = 0$). The major differences between the curves are more noticeable from the four-seconds mark onwards. Additionally, the steady condition is achieved after about thirty seconds and no major change happens after this time stamp. The same results were also extracted for the fuel rod exit analysis ($z = 2.1336m$) and can be seen on Figure 5.a and 5.b, similar behavior can be observed, although with small temperature gradients. This becomes evident when figure 4.b shows a temperature difference of 100 K between the centered pellet curve and pellet shifted 0.07 mm curve while in Figure 5.b this is about 10 K.

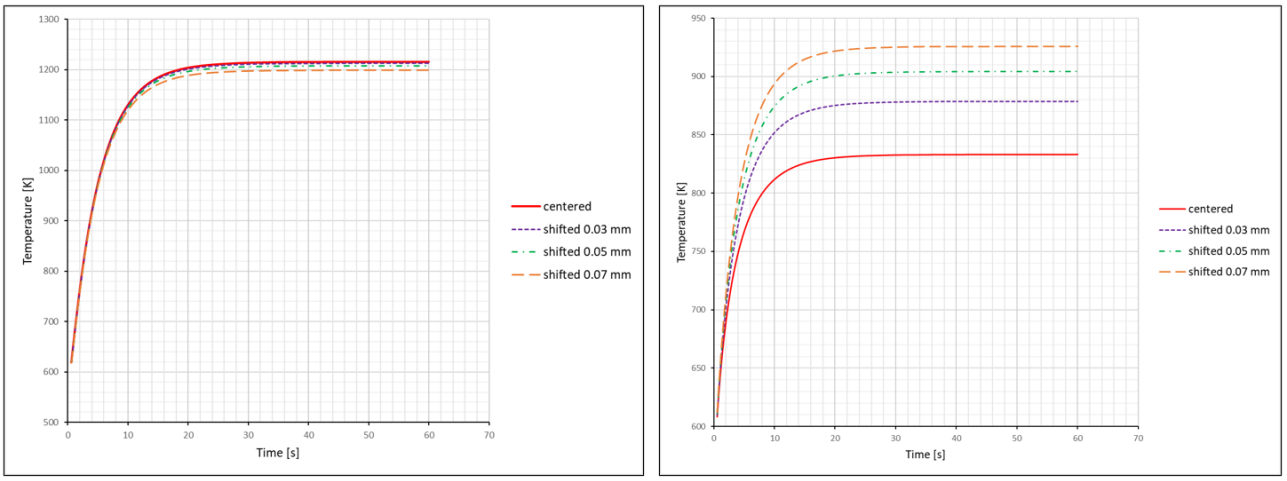

(a) (b)

Figure 4. (a) Max. Temperature over time on pellet for the fuel rod center ($z = 0$), and (b) Max. Temperature over time on pellet wall for the fuel rod center ($z = 0$).

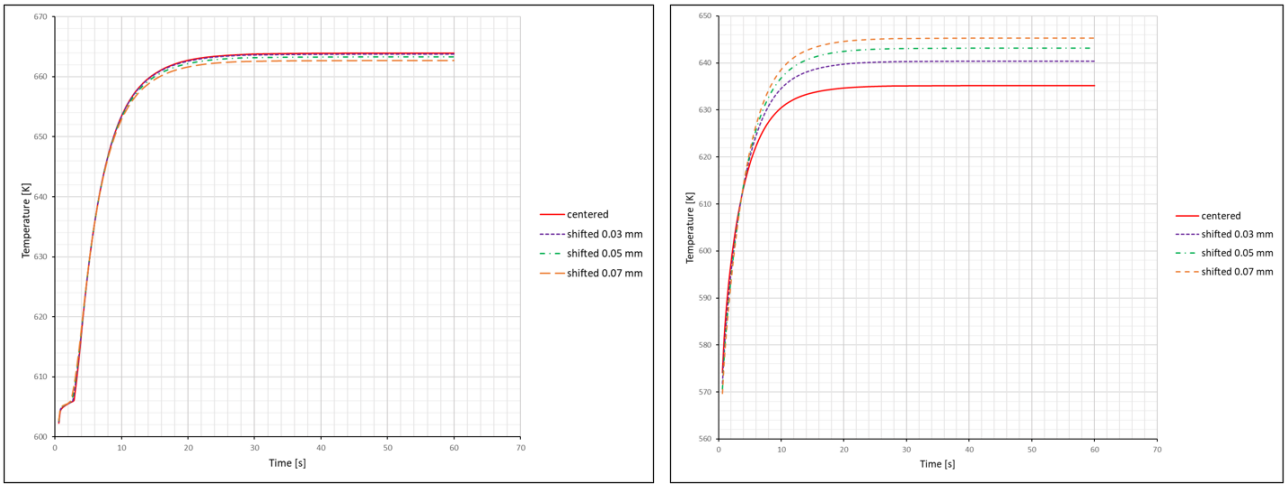

Figure 5. (a) Max. Temperature over time on pellet for the fuel rod exit ($z = 2.1336m$), and (b) Max. Temperature over time on pellet wall for the fuel rod exit ($z = 2.1336m$).

5. CONCLUSIONS

This study evaluated the influence of fuel pellet displacement on the temperature distribution of a fuel rod from an AP1000 reactor using the FEM technique. The temperature profile in the radial direction provides information on how the pellet shift can change the temperature in the pellet wall and how it can influence the maximum temperature of the inner and outer surface of the cladding. When the pellet is radially shifted, the maximum temperature change occurs on the pellet, with no significant impact on the fuel cladding. Additionally, a maximum temperature spot shift inside the fuel and the decrease of the maximum temperature registered on the fuel pellet could be noted as result of the modified thermal resistance of the gap. Furthermore, the transient analysis showed consistent results in comparison to steady-state analysis. Results provided by this analysis can be the focus of future thermal structural analysis to evaluate the stress-induced on the fuel by the differential thermal expansion and also to a result comparison with an analysis conducted on finite volume by a Computer Fluid Dynamics approach (CFD).

6. REFERENCES

Bejan, A., 1993. *Heat Transfer 1st Edition,* John Wiley & Sons, New York, United States.

Costa, R.Y.N., 2017. *Two-dimensional Thermal Analysis of a Nuclear Fuel Pin By The Finite Volumes Method Under Variable Neutronic Flow* (in Portuguese). Master's Thesis, Postgraduate Program in Energetic and Nuclear Technologies, Federal University of Pernambuco, Pernambuco, Brazil.

D'Ambrosi, V., Destouches, C., Ricciardi, G., Breaud, S., Lebon, F., Gatt, J.M., Julien, J., Parrat, D., 2021. *Fuel rod nonlinear vibrations to detect and characterize Pellet-Cladding Interaction.* Nuclear Engineering and Design, Vol. 379, p. 111214.

El-Wakil, M. M., 1971. *Nuclear Heat Transport. Scraton, PA: International Textbook Company.*

Fenech, H., 1981. *Heat Transfer and Fluid Flow in Nuclear Systems.* Pergamon Press, Oxford, UK.

Hagrman, D.T., 1995. *SCDAP/RELAP5/MOD 3.1 code manual: MATPRO, A library of materials properties for Light-Water-Reactor accident analysis.* Office of Scientific & Technical Information Technical Reports, Vol. 4.

IAEA, 2006. *Thermophysical Properties Database of Materials for Light Water Reactors and Heavy Water Reactors.* International Atomic Energy Agency, Vienna, Austria.

Incropera, F.P., DeWitt, D.P., Bergman, T.L. and Lavine, A.S., 2008. *Fundamentals of Heat and Mass Transfer 6th Edition*, LTC Rio de Janeiro. Brasil.

Kok, K.D., 2017. *Nuclear Engineering Handbook 2nd Edition*, CRC Press, Boca Raton, United States.

Lamarsh, J.R. and Baratta, A.J., 2001. *Introduction to Nuclear Engineering 3rd Edition*, Prentice Hall, New Jersey, United States.

Lanning, D.D., Hann, C.R., 1975. *Review of methods applicable to the calculation of gap conductance in zircaloy-clad uo2 fuel rods*, Battelle Pacific Northwest Labs, Washington, United States.

Lucuta, P.G., 1996. *A pragmatic approach to modelling thermal conductivity of irradiated UO2 fuel: Review and recommendations.* Journal of Nuclear Materials, Vol. 232, p. 166 - 180.

Martin, D.G., 1988. *The Thermal Expansion of Solid UO2 and Mixed Oxides — A Review and Recommendations.* Journal of Nuclear Materials, Vol. 152, p. 9 - 101.

Mihaila, B., Stan, M., Ramirez, J., Zubelewicz, A., and Cristea, P., 2009. *Simulations of coupled heat transport, oxygen diffusion, and thermal expansion in UO2 nuclear fuel elements.* Journal of Nuclear Materials, Vol. 394, p. 182–189.

Newman, C., 2009. *Three dimensional coupled simulation of thermomechanics, heat, and oxygen diffusion in UO2 nuclear fuel rods.* Journal of Nuclear Materials, Vol. 359, p. 174 - 184.

NIST, 2021. Thermophysical Properties of Fluid Systems. https://webbook.nist.gov/chemistry/fluid/. Accessed 15 June 2021.

Tang, J., Huang M., Zhao, Y., Ouyang, X., Huang, J., 2017. *A new procedure for solving steady-state and transient-state nonlinear radial conduction problems of nuclear fuel rods.* Annals of Nuclear Energy, Vol. 110, p.492 - 500.

Todreas, N.E. and Kazimi, M.S. 2011. *Nuclear Systems: Thermal Hydraulic Fundamentals*, CRC Press, Florida, United States.

Westinghouse, 2011. *AP1000 European Design Control Document: Revision 19*, Westinghouse Electric Company LLC.

Westinghouse, 2016. *Optimized ZIRLO: High Performance Fuel Cladding Material*, Westinghouse Electric Company LLC.

7. Responsibility notice

The authors Felipe F. Timoteo, Thiago F. Ribeiro Dias da Rosa and Marcos F. Curi are the only ones responsible for the printed material included in this paper.